

RESEARCH PAPER

# Epoxy Resin Containing Carbon Nanotubes and Nickel Ferrite Nanoparticles to Increase Thermal Stability and Flame Retardancy

Maryam Asadi, Mojtaba Goodarzi \*, Davood Ghanbari

Department of Science, Arak University of Technology, Arak, Iran

## ARTICLE INFO

### Article History:

Received 14 April 2022

Accepted 27 June 2022

Published 01 July 2022

### Keywords:

Hydrothermal

Flammability

Nanotubes

Retardant Properties

Thermal Resistance

## ABSTRACT

In this work thermal stability and flame-retardancy of epoxy polymer have been considered. Nickel ferrite nanoparticles were fabricated using ultra-sonic waves and these nanoparticles with modified carbon nanotubes were added to epoxy resin. In order to study size and morphology of the produced samples scanning electron microscopy (SEM), was studied. Also for better investigation of shape, particle and nanotubes size transmission electron microscope (TEM) was applied. X-ray diffraction pattern illustrate phase of the nickel ferrite product, Fourier transform infra-red (FT-IR) confirm purity and bonds in the compound. Thermal gravimetric analysis approve improving thermal stability of the product in the presence of modified carbon nano tubes. Also UL-94 test confirm increasing flame retardancy of the product by addition of nickel ferrite nanoparticles. This magnetic char as a barrier decrease reaching of oxygen, flame and heating to the protected under side polymer.

## How to cite this article

Asadi M, Goodarzi M, Ghanbari D. Epoxy Resin Containing Carbon Nanotubes and Nickel Ferrite Nanoparticles to Increase Thermal Stability and Flame Retardancy. J Nanostruct, 2022; 12(3):557-562. DOI: 10.22052/JNS.2022.03.008

## INTRODUCTION

Nanotechnology is an interdisciplinary science in between pure research and industrial activity which grows rapidly in different fields. Nickel ferrite ( $\text{NiFe}_2\text{O}_4$ ) with reverse spin structure, soft magnetic property, has high electrical resistance characteristics [1-3]. For this reason, it has many applications in industry. Today, the use of nanotechnology to delay combustion and increase the fire resistance of materials is common. The production of polymer nanocomposites and the use of some additives have increased the strength of the polymer against flammability [4-8]. In the obtaining desired characteristics, the choice of synthesis technique is a fundamental stage in the final product with the chemical, physical, structural

and magnetic properties of a spinel ferrite. Among different methods used in the production of magnesium ferrite nanoparticles, the hydrothermal and sono Chemistry methods were applied in this study because of they are simple synthesis and low cost [9-14]. In this work, epoxy resin was used to increase the resistance of the material against flammability. The carbon nanotube structures composed of epoxy resins produced with nickel ferrite show both magnetic and heat-resistant properties. This article will be presented in four sections, introduction, experimental section, which explains the fabrication of nanoparticles and carbon nanotubes, the section reviewing the analyzes performed using the results obtained, and finally the conclusions obtained.

\* Corresponding Author Email: [m.goodarzi@arakut.ac.ir](mailto:m.goodarzi@arakut.ac.ir)



## MATERIALS AND METHODS

Ni(NO<sub>3</sub>)<sub>2</sub>·6H<sub>2</sub>O, Fe(NO<sub>3</sub>)<sub>3</sub>·9H<sub>2</sub>O, NaOH, were provided from Merck Company.

By an X-ray diffractometer (Ni-filtered) Cu-Kα radiation in the wide range of 2θ (10° < 2θ < 80°) (Phillips Expert Pro PW3040) X-ray diffraction (XRD) patterns were recorded. Scanning electron microscopy (SEM) images were obtained using a KYKY of model EM3200. Before taking the images, all products were coated by a layer of Au to create conductivity on the sample surface for the prevention of the accumulation of electronic charge, and creating a good contrast. Transmission Electron Microscopy images were prepared by JEOL microscope.

The field emission scanning electron microscopy (FESEM) of model MIRA3TESCAN-XMU, was utilized for energy dispersive X-ray spectroscopy (EDS) and X-ray element distribution maps (MAP) analysis. Fourier transform infrared (FT-IR) spectra with the range of 400–4000cm<sup>-1</sup> with a resolution of 1cm<sup>-1</sup> were obtained by a Bruker spectrometer. Potassium bromide was applied for the sample preparation. The magnetic properties of the specimens were evaluated at room temperature using a vibrating sample magnetometer (VSM) device, made by Meghnatis Daghighi Kashan Company in magnetic field (between ±10000 Oe).

A Bunsen burner flame is applied to the specimen for a UL-94 test. The mechanical properties of the films were investigated with tensile tests using a Zwick Roell Pro Line Z010 machine. Specimens with a thickness of 1mm were tested according ASTM D638 standard at the speed of 0.5mm/min. All tests were repeated five times.

### Synthesis of NiFe<sub>2</sub>O<sub>4</sub> nanoparticles

In this experiment, we have prepared Nickel ferrite applying the hydrothermal method. 0.25g of Ni(NO<sub>3</sub>)<sub>2</sub>·6H<sub>2</sub>O and 0.7g of Fe(NO<sub>3</sub>)<sub>3</sub>·9H<sub>2</sub>O were dissolved in 200mL of Distilled water. The resulting solution was mixed at 70 ° C for 40 minutes. Then NaOH slowly added to the resulting clear solution, the resulting solution turns crimson at ambient temperature. The solution is then placed in an autoclave at 180 ° C for 5 hours. After 5 hours, remove the material and centrifuge for 2 minutes. Finally, the resulting material is placed in an oven at 70 ° C for 24 hours to dry.

## RESULTS AND DISCUSSION

### XRD analysis

To identify the phase and structural analysis and to obtain the approximate size of crystallite, the synthesized samples were subjected to

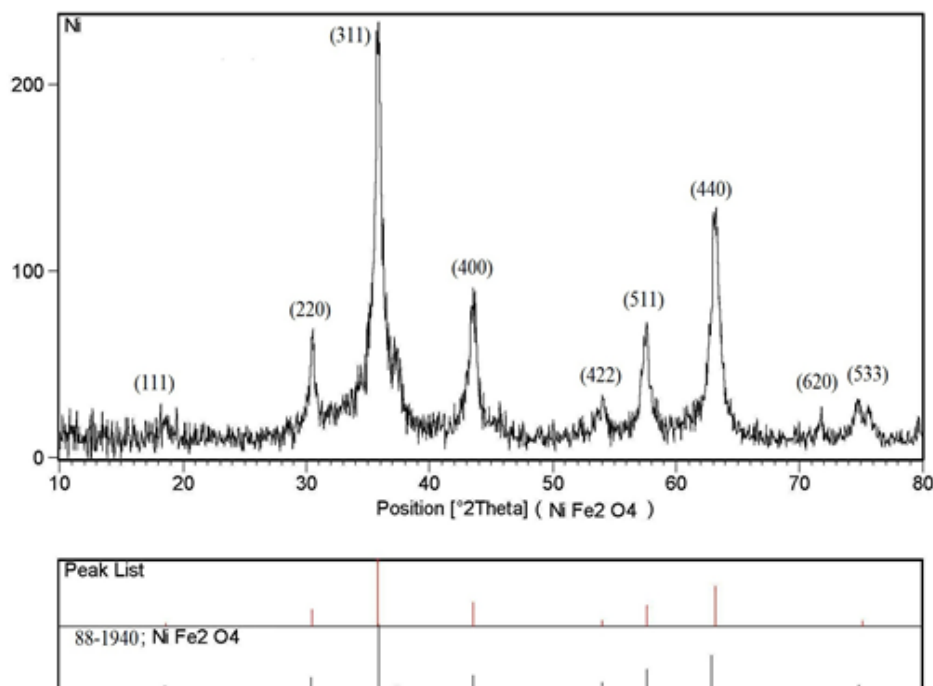


Fig. 1. X-ray diffraction pattern of NiFe<sub>2</sub>O<sub>4</sub> nanoparticles

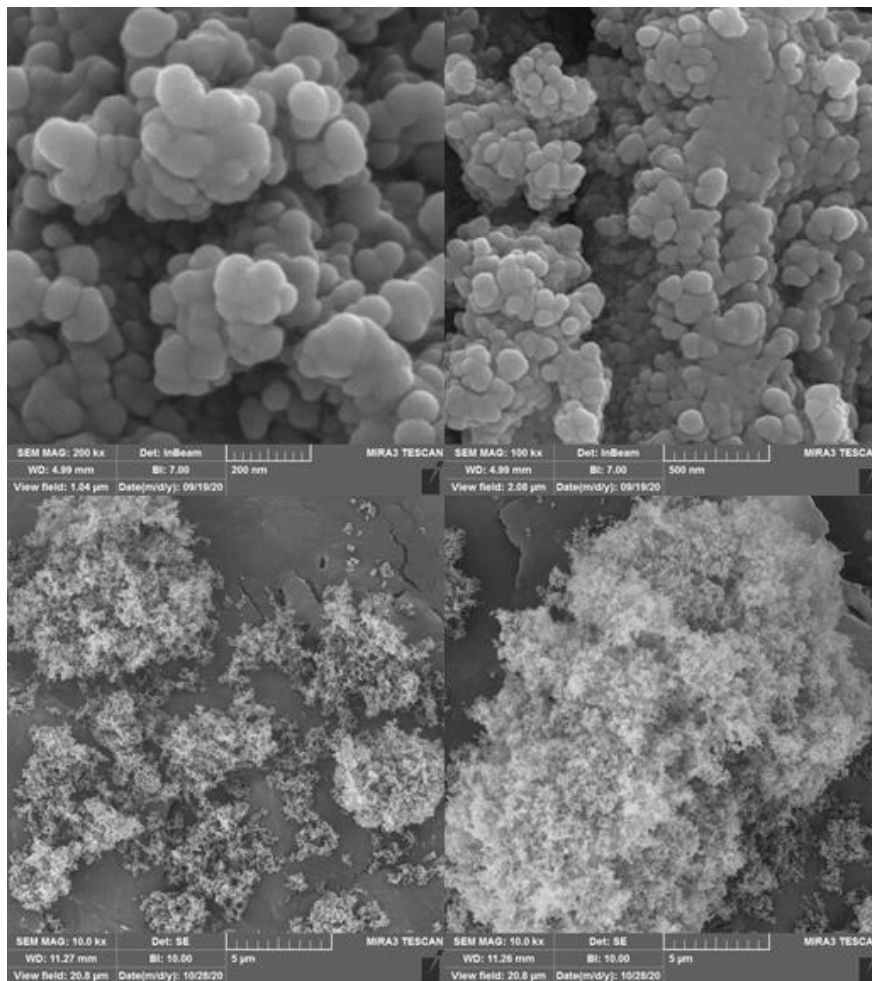


Fig. 2. SEM images of theas-obtained NiFe<sub>2</sub>O<sub>4</sub> nanoparticles

X-ray diffraction analysis. Fig. 1 shows the X-ray diffraction pattern of NiFe<sub>3</sub>O<sub>4</sub> nanoparticles, the crystal structure of the fabricated nanoparticles had a cubic phase with the space group Fd-3m. (space group: Fd-3m, JCPDS No. 88-1940). The intensity and sharpness of the peak in the direction orientation (311) is due to the very good crystallinity of the nanoparticles. The crystal size is calculated using the Debye-Scherrer ratio and the average size of the crystals is approximately 20 nm.

SEM was applied for the evaluation of the morphology and particle size of the products. SEM images of Nickel ferrite prepared in the presence in Fig. 2. The images confirm the preparation of nanostructures with an average size of less than 100 nm.

SEM images of carbon nano tube prepared in

the presence in Fig. 3. The images confirm the preparation of nanostructures with an average size of less than 100 nm

In this study, a transmission electron microscope was used to investigate more details and microstructure of materials and higher resolution, which is due to the better resolution of the short wavelength of the electrons used for exposure in these microscopes.

The image of carbon nanotubes is presented by a passing electron microscope in Fig. 4. In the mentioned figure, the hollowness of the nanotubes was clearly observed and also the nanotubes were connected in the form of strands and chains so that the average diameter of each strand was about 15 nanometers and had a length of about a few micrometers.

The FT-IR image of nickel ferrite nanoparticles

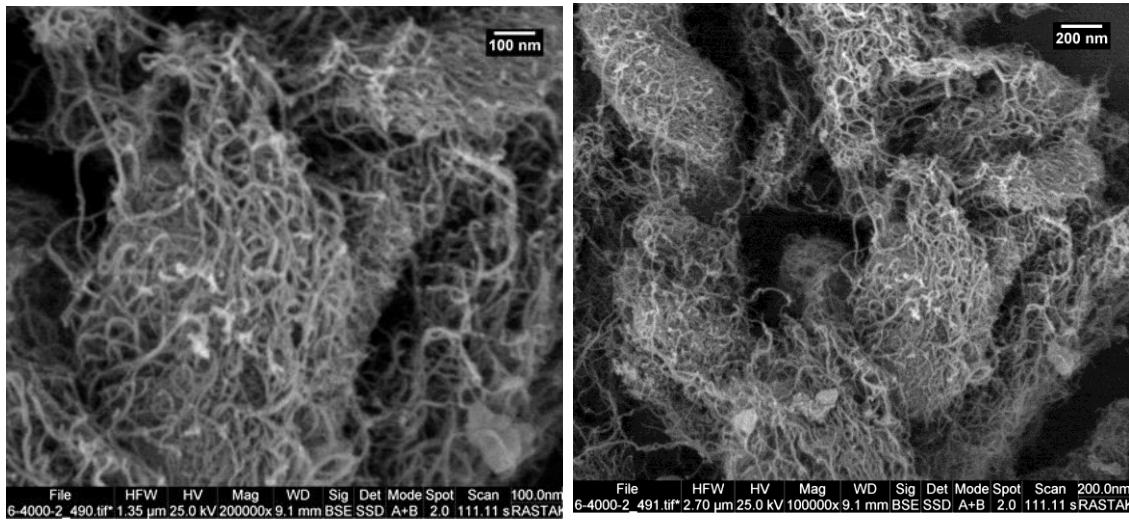


Fig. 3. SEM images of carbon nanotubes

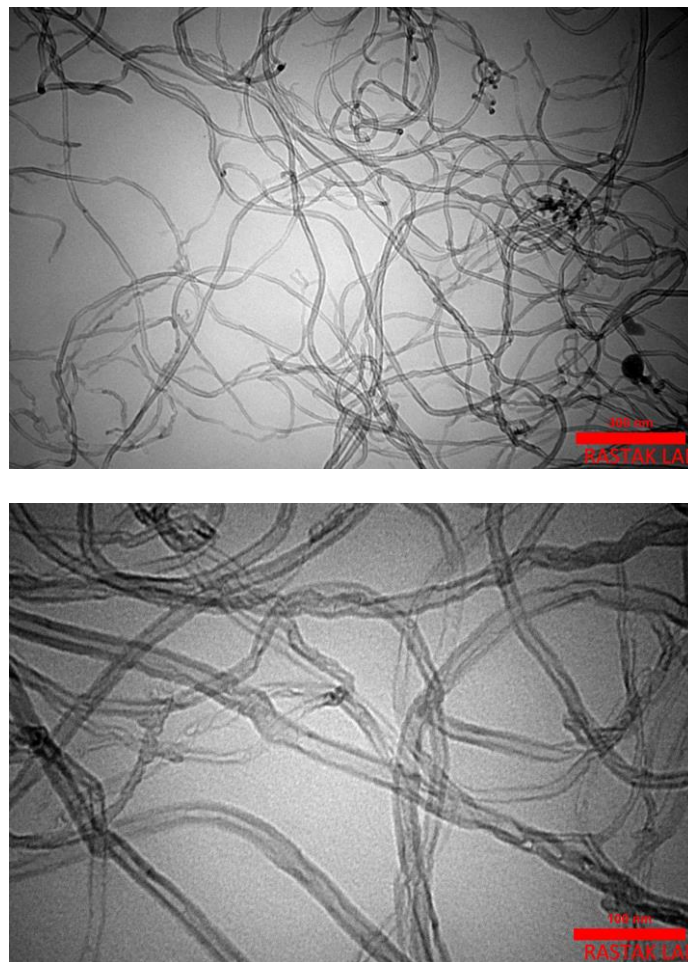


Fig. 4. TEM analysis of the carbon nanotubes

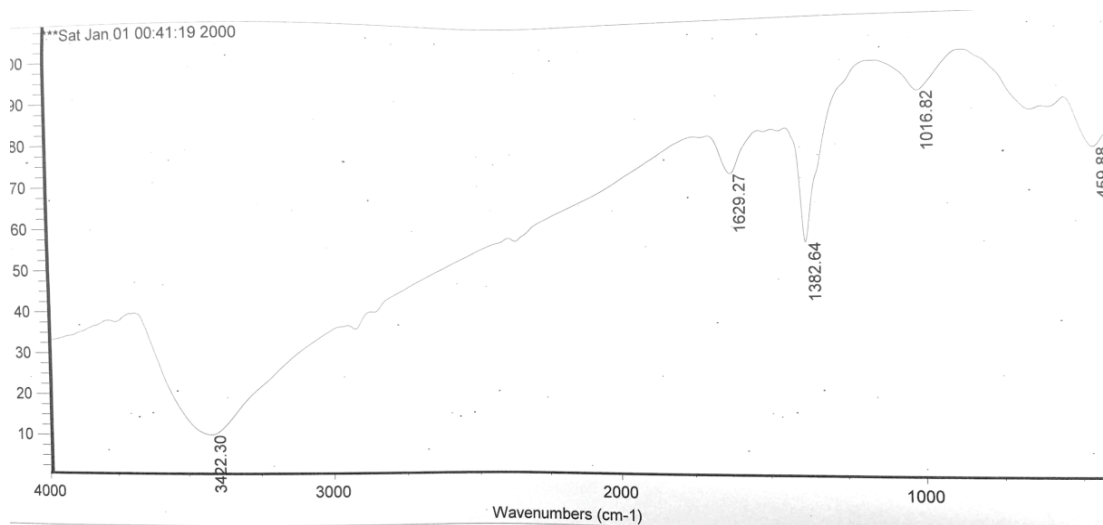


Fig. 5. FT-IR spectrum NiFe<sub>2</sub>O<sub>4</sub> nanoparticles



Fig. 6. UL-94 test of prepared nanocomposite

made is presented in Fig. 5. In the diagram below, where the percentage of adsorption (Transmittance%) is plotted in terms of wave number (cm<sup>-1</sup>), it can be seen that the adsorption in the range of 400 to 600 cm<sup>-1</sup> is related to the iron-oxygen and nickel-oxygen bond and In the range of 3300 to 3500 cm<sup>-1</sup>, there is a peak that indicates the hydroxyl adsorbed on the nickel ferrite nanoparticles. In this spectrum, due to the absence of a sharp peak of impurities, the sample was of acceptable purity.

#### Evaluation of Flame retardancy

The ferrite effect on the flame retardancy was tested applying UL-94 test. If it shut down in time less than 10s (after fire application) categorized

as V-0, (drips are accepted since they are not blazing.) A V-1 classification is for a specimen when maximum ignition time less than 30s (drips are like V-0 condition). The sample is arranged V-2 similar situation was happened while flaming drips are permitted. Samples are categorized non classified. In UL-94 when the maximum total combustion time is more than 50s. The specimen is ordered HB when slow firing on a horizontal sample; burning rate less than 74 mm/min. The UL-94 outcomes for Epoxy and epoxy nanocomposite are non classified and V-0 respectively. Nanostructures act as block layer; this magnetic obstacle layer inhibits oxygen reaching. Hydroxyl groups on the surface of ferrite have appropriate interaction with hydroxyl groups of epoxy. Nanoparticles suitably

disperse in polymer matrix. Under flame, magnetic nanostructures stand together durable to collapse and build a dam. This inhibitor slow volatilization of organic fragments and preclude heat and flame affecting to the surface of the nanocomposite.

## CONCLUSION

Nickel Ferrite nanostructures were successfully synthesized via a fast auto-combustion reaction by applying fruit extracts. Nanoparticles were characterized using XRD, SEM and TEM techniques. The effect of various green extracts on the morphology of the products was studied.

## CONFLICT OF INTEREST

The authors declare that there is no conflict of interests regarding the publication of this manuscript.

## REFERENCES

1. Chandradass J, Jadhav AH, Kim KH, Kim H. Influence of processing methodology on the structural and magnetic behavior of  $\text{MgFe}_2\text{O}_4$  nanopowders. *J Alloys Compd.* 2012;517:164-169.
2. Foroughi F, Hassanzadeh-Tabrizi SA, Bigham A. In situ microemulsion synthesis of hydroxyapatite- $\text{MgFe}_2\text{O}_4$  nanocomposite as a magnetic drug delivery system. *Materials Science and Engineering: C.* 2016;68:774-779.
3. Maensiri S, Sangmanee M, Wiengmoon A. Magnesium Ferrite ( $\text{MgFe}_2\text{O}_4$ ) Nanostructures Fabricated by Electrospinning. *Nanoscale Research Letters.* 2008;4(3).
4. Patil J, Nadargi D, Mulla IS, Suryavanshi SS. Spinel  $\text{MgFe}_2\text{O}_4$  thick films: A colloidal approach for developing gas sensors. *Mater Lett.* 2018;213:27-30.
5. Iravani S. Green synthesis of metal nanoparticles using plants. *Green Chem.* 2011;13(10):2638.
6. Ahmed S, Ahmad M, Swami BL, Ikram S. A review on plants extract mediated synthesis of silver nanoparticles for antimicrobial applications: A green expertise. *Journal of Advanced Research.* 2016;7(1):17-28.
7. Diodati S, Pandolfo L, Caneschi A, Gialanella S, Gross S. Green and low temperature synthesis of nanocrystalline transition metal ferrites by simple wet chemistry routes. *Nano Research.* 2014;7(7):1027-1042.
8. Chandra Babu Naidu K, Madhuri W. Microwave Hydrothermal Synthesis: Structural and Dielectric Properties of nano  $\text{MgFe}_2\text{O}_4$  Ceramics. *Materials Today: Proceedings.* 2016;3(10):3810-3813.
9. Hussein SI, Elkady AS, Rashad MM, Mostafa AG, Megahid RM. Structural and magnetic properties of magnesium ferrite nanoparticles prepared via EDTA-based sol-gel reaction. *J Magn Magn Mater.* 2015;379:9-15.
10. Benslimane A, Bahlouli IM, Bekkour K, Hammiche D. Thermal gelation properties of carboxymethyl cellulose and bentonite-carboxymethyl cellulose dispersions: Rheological considerations. *Applied Clay Science.* 2016;132-133:702-710.
11. Javanbakht S, Pooresmaeil M, Hashemi H, Namazi H. Carboxymethylcellulose capsulated Cu-based metal-organic framework-drug nanohybrid as a pH-sensitive nanocomposite for ibuprofen oral delivery. *Int J Biol Macromol.* 2018;119:588-596.
12. Feng J, Carpanese C, Fina A. Thermal decomposition investigation of ABS containing Lewis-acid type metal salts. *Polymer Degradation and Stability.* 2016;129:319-327.
13. Yousefi M, Gholamian F, Ghanbari D, Salavati-Niasari M. Polymeric nanocomposite materials: Preparation and characterization of star-shaped PbS nanocrystals and their influence on the thermal stability of acrylonitrile-butadiene-styrene (ABS) copolymer. *Polyhedron.* 2011;30(6):1055-1060.
14. Ghanbari D, Salavati-Niasari M, Ghasemi-Kooch M. In situ and ex situ synthesis of poly(vinyl alcohol)- $\text{Fe}_3\text{O}_4$  nanocomposite flame retardants. *Particuology.* 2016;26:87-94.
15. Abdi Z, Maghazeei F, Ghanbari D. The Effect of Calcium Perovskite and Newly Developed Magnetic  $\text{CaFe}_2\text{O}_4/\text{CaTiO}_3$  Perovskite Nanocomposite on Degradation of Toxic Dyes Under UV-Visible Radiation. *Journal of Cluster Science.* 2021:1-3.
16. Kiani A, Nabiyouni G, Masoumi S, Ghanbari D. A novel magnetic  $\text{MgFe}_2\text{O}_4$ - $\text{MgTiO}_3$  perovskite nanocomposite: rapid photo-degradation of toxic dyes under visible irradiation. *Composites Part B: Engineering.* 2019;175:107080.
17. Maghazeei F, Ghanbari D. The Study of Nanostructure, Magnetic Properties and Photocatalytic Behavior of  $\text{Fe}_3\text{O}_4/\text{Ag}$  Nanocomposites Synthesized by Microwave Method. *Advanced Materials and New Coatings.* 2020;9(34):2462-73.